

STUDY ON SEISMIC BEHAVIOR OF RC COMPOSITE CORE WALLS WITH CONCEALED STEEL TRUSS SUBJECTED TO COMBINED ACTION

CAO Wanlin¹, CHANG Weihua², ZHANG Jianwei¹

¹ College of architecture and Civil Engineering, Beijing University of Technology, Beijing, China

² China Academy of Building Research, Beijing, China

Email:changweihua@cabrtech.com

Abstract: In this paper, reinforced concrete composite core wall with concealed steel truss were proposed. This new composite core wall includes two kinds of composition. One is composition of two bearing systems, including truss and core wall, the other is composition of two materials, including steel and concrete. Two 1/6 scale core walls specimens were designed, including a normal reinforced concrete core wall and a reinforced concrete composite core wall with concealed steel truss. The experimental study on the seismic behavior of two core walls subjected to combined action of compression, bending moment, shear and torque, was carried out. The load-carrying capacity, stiffness, ductility, hysteretic behavior, energy dissipation and failure mechanism of the core walls were discussed. The test results showed that the seismic performance of core walls was improved greatly by the concealed steel truss. Based on the rotating-angle softened truss model theory, this paper presents a three-dimensional model for analysis of reinforced concrete composite core walls with concealed steel truss subjected to complex loading. Through the results of calculation coincided with the test well, this model can predict the ultimate strength of the load-carrying capacity of reinforced concrete composite core walls with concealed steel truss, and provide a tool to obtain the entire load-deformation history.

Key words: steel truss, reinforced concrete core walls, combined action, seismic performance, nonlinear analysis

1. INTRODUCTION

With the progress of Chinese urbanization accelerated, more and more high-rise buildings have been set up in the cities. It's believed that China is much more likely to be stricken by earthquakes. How to improve the seismic behavior of the core wall with restricted thickness has become a key problem of seismic design. Concealed steel truss is able to greatly improve seismic performance of normal shear wall and core wall (Cao et al, 2003, 2004, 2005,2007). The experiment and research show SRC shear walls have good yielding ability (Anwar Hossain et al,2004. Driver et al,1998. Hossain,2004)In this paper, the author tries to propose that concealed steel truss could be added in shear core to increase the seismic performance of it.

2. EXPERIMENTAL DETAIL

In order to investigate the seismic performance of RC core wall with concealed steel truss, two core walls are designed. The test specimens are labeled as CWT-1 and CWT-2, respectively. Where CWT-1 is the normal RC core wall without concealed steel truss; CWT-2 is the RC core wall with concealed steel truss while maintaining the main reinforcement of CWT-1. The dimensions of specimen CWT-1 is the same as specimen CWT-2. Two specimens are both symmetric construction. The shear span ratio of both specimens is 2.1. Specimens are three layers of the bottom of core wall. The height for first and second layer are 830 mm, and the height for the third layers is 600 mm, and height of based were 360 mm, and the thickness of the loaded plate at the top was 300 mm, and the distance from the loading point to the surface of model based was 2260 mm, and the height of the specimen was 2770 mm. The thickness of the coupling wall-column is designed as 75mm.

Specimens are poured with fine-stone concrete. Concrete strength grade is designed as C35 and the average of the measured cube concrete compressive strength of CWT-1 and CWT-2 is 44.1 MPa, 42.4 MPa respectively. Mechanical properties of steel bars are tabulated in Table 1. Schematic view of test set-up is illustrated in Figure 1, and Schematic view of displacement gauges is illustrated in Figure2. The dimensions and reinforcement details for specimen CWT-1 is illustrated in Figure3. The dimensions and reinforcement details for specimen CWT-1 is illustrated in Figure4.

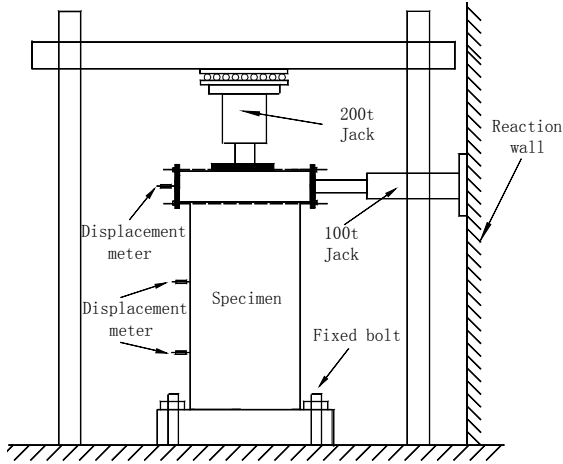


Fig.1 Schematic view of test set-up

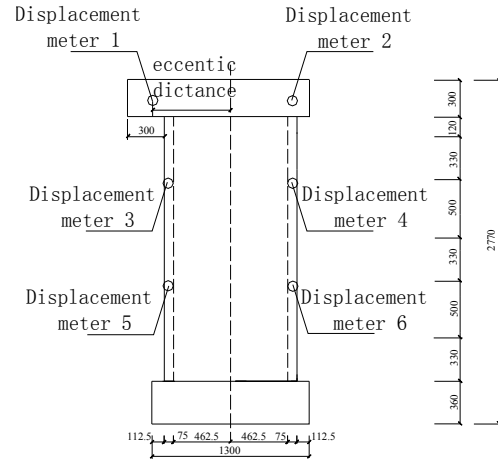


Fig.2 Schematic view of displacement gauges

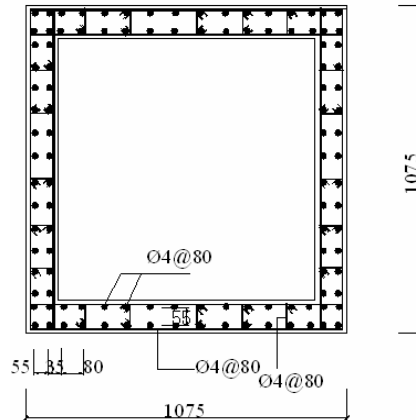
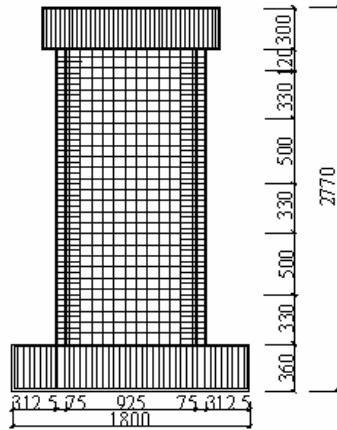


Fig.3 Geometry and reinforcement details of specimen CWT-1

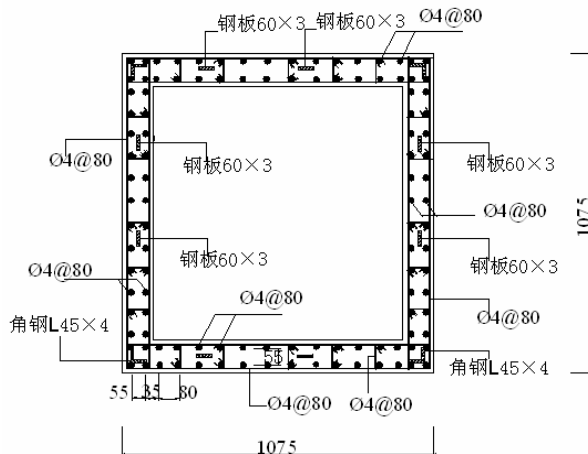
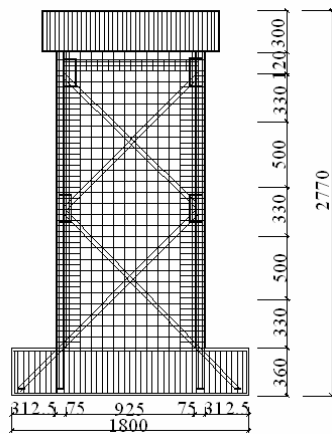


Fig.4 Geometry and reinforcement details of specimen CWT-2
Table1 Mechanical properties of steel bar and profiled steel

Steel Bar and Profiled Steel	Yield Strength f_y /MPa	Ultimate Strength f_b /MPa	Elongation Rate /%	Elasticity Modulus /MPa
8# iron wire	370	448	15.0	1.96×10^5
ϕ b4 Steel Bar	669	836	7.5	2.06×10^5
L 45×4 Profiled Steel	327	463	28.3	2.10×10^5
60×3 Steel Plate	314	448	30.3	1.96×10^5

During experiment, the vertical axial load was imposed at the top of model through vertical jack, and the vertical beam connected with the vertical jack through the rolling bearings. The vertical pressure was 1320kN, and regulator system used to maintain its value remains unchanged, after vertical axial load was imposed. A low-frequency cyclic loading is horizontally applied at verge of loaded plate of specimen by a push and pull jack. The specimens were subjected to eccentric horizontal loading. The distance from the displacement gauges to wall base is 2260mm, 1660mm, 830mm respectively. Axial loads for specimen CWT-1 and specimen CWT-2 are 1320kN.

All the stains, displacements and loads are recorded and analyzed by IMP data gathering system connected to the specimen. The cracking of the specimen is monitored during the experiments.

3 EXPERIMENTAL RESULTS AND ANALYSIS

3.1 Load-Carrying Capacity

The measured loads corresponding to concrete cracking, effective yielding of the section and ultimate load-carrying capacity of the specimen are tabulated in Table 2, where F_c is concrete cracking load which is the measured load corresponding to the first concrete crack; T_c is concrete cracking torque which is the measured load corresponding to F_c ; F_y is yield load which is defined as the average of positive load and negative load, since positive yield load is close to negative yield load; T_y is yield torque which is corresponding to F_y ; F_u is ultimate load which is the maximum horizontal load applied to the specimen; Since the specimens are symmetrical structure, F_u is defined as the average of positive load and negative load; T_u is ultimate torque which is corresponding to F_u and $\mu_{yu} = F_y/F_u = T_y/T_u$, represents the ratio of yield strength to ultimate strength.

Table 2 Experimental results of carrying-load capacity

Specimen	Concrete Cracking Load			Yield Load			Ultimate Load			Ratio of Yield to Ultimate	
	F_c /kN	T_c /kN·m	Relative Value	F_y /kN	T_y /kN·m	Relative Value	F_u /kN	T_u /kN·m	Relative Value	μ_{yu}	Relative Value
CWT-1	235.14	148.73	1.000	358.50	226.75	1.000	506.39	320.29	1.000	0.708	1.146
CWT-2	240.25	151.96	1.022	398.45	252.02	1.112	644.86	407.87	1.273	0.618	1.000

It is observed from Table 2 that:

- (1) Compared with the normal core wall, the cracking load is slightly increased by adding the concealed steel truss within the wall.
- (2) Compared with the normal core wall, the yield load and ultimate load are all significantly increased by adding the concealed steel truss within the wall. The measured yield load and ultimate load for CWT-2

are increased respectively by 11.2% and 27.3% in comparison with the specimen CWT-1.

- (3) Compared with the normal core wall, the ratio of yield strength to ultimate strength is significantly increased by 14.6%.

3.2 Stiffness

The measured stiffness and stiffness degradation coefficients for the test specimens are tabulated in table 3. Where K_0 is the initial tangent stiffness; K_c is the secant stiffness corresponding to the cracking state of the wall; K_y is the secant stiffness corresponding to the yield state of the wall; $\beta_{c0} = K_c / K_0$ represents the stiffness degradation coefficient from the initial elastic state to the cracking state; $\beta_{yc} = K_y / K_c$, representing the stiffness degradation coefficient from the cracking state to the yielding state; $\beta_{y0} = K_y / K_0$ represents the stiffness degradation coefficient from the initial elastic state to the yielding state.

The following observations can be made from Table 3:

- (1) Specimen CWT-1 and Specimen CWT-2 have almost the same initial elastic stiffness K_0 .
- (2) Specimen CWT-1 and Specimen CWT-2 have almost the same cracking stiffness K_c . The data indicate that in initial state stiffness is determined by concrete strength and specimen dimension and concealed steel truss does not have much effect on stiffness K_0 and K_c .
- (3) The yield stiffness K_y for the core wall with concealed steel truss shows a significant increase over that for the core wall without concealed steel truss. This can be explained by the concealed steel truss embedded in the core wall restricting the expanding of concrete cracks and resulting in the stiffness slower degrading. It is seen from all state of experiment that the stiffness in final stage is more stable for the core wall with concealed steel truss, which is more favorable for seismic resistance.
- (4) Compared with the normal core wall, the value of β_{yc} are all significantly increased by adding the concealed steel truss within the wall.
- (5) Compared with the normal core wall, the value of β_{y0} is significantly increased by 13.4%.

Table 3 Measured stiffness and stiffness degradation coefficients

Specimen	K_0 /kN·mm ⁻¹	K_c /kN·mm ⁻¹	K_y /kN·mm ⁻¹	β_{c0}	β_{yc}	β_{y0}	β_{y0} Relative Value
CWT-1	221.50	123.44	40.68	0.557	0.330	0.184	1.000
CWT-2	225.86	128.37	47.04	0.568	0.366	0.208	1.134

3.3 Ductility

The measured displacement and ductility ratios for the test specimens are listed in table 4, where all the displacements are measured at the top plate of the core wall. u_c is the displacement at the cracking state; u_y is the displacement at the yielding state; u_d is the positive ultimate displacement of the specimen; and $\mu = u_d / u_y$ is defined as the ductility ratio of the shear wall (u_d is calculated with positive value in this paper).

It is observed from Table 4 that:

- (1) The yielding displacements for specimens with concealed steel truss show a little increase over that for the specimens without concealed steel truss.
- (2) The ultimate displacements are significantly increased for the core walls with concealed steel truss.
- (3) The ductility ratio for specimen CWT-2 is increased by 20.4% in comparison with specimen CWT-1.

Therefore, the ductile behavior of the core wall can be significantly improved by setting concealed steel

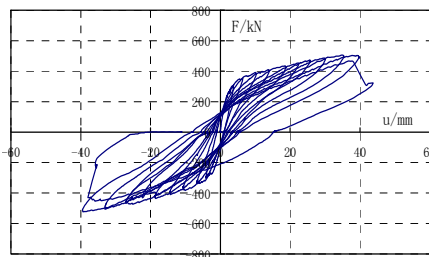
truss within the core wall.

Table 4 Experimental results of displacement and ductility coefficient

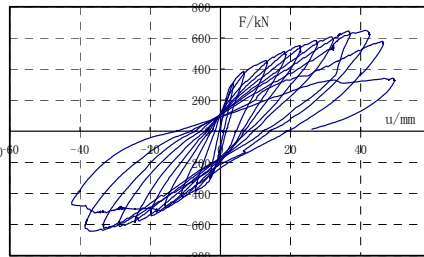
Specimen	u_y/mm			u_d/mm			μ	μ Relative Value	θ_p	θ_p Relative Value
	positive	negative	average	positive	negative	average				
CWT-1	8.92	8.71	8.82	40.19	37.42	38.81	4.40	1.000	1/58	1.000
CWT-2	9.32	8.92	8.47	48.7	41.06	44.88	5.30	1.204	1/50	1.160

3.4 Hysteretic Behavior and Energy Dissipation Capacity

The measured load-displacement hysteresis loops for the specimens are shown in Figure 5. And comparative skeleton curve of positive loading are shown in Figure 6. It is seen that the hysteresis loops for the specimen CWT-2 is wider than that of CWT-1. The core walls with concealed steel truss present larger inner hysteresis loop areas than the normal core walls without concealed steel truss. The core walls with concealed steel truss, therefore, provide better energy absorbing capacity. It is also noticed that the core walls with concealed steel truss exhibit better plastic deformation capacity and ductility and their load-carrying capacity is also increased.



(a) CWT-1



(b) CWT-2

Figure 5. Measured hysteresis loop

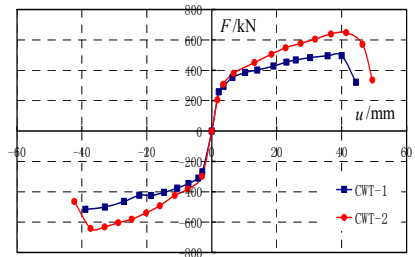


Figure 6. Skeleton curve of positive loading

The elastic-plastic energy dissipation capacity of the specimens can be evaluated using the inner area of the hysteresis loop. The greater the inner area is the better the energy dissipation capacity will be. In analysis described in this paper, the area in the first and third quadrant of the hysteresis loop is approximately computed and used as an index of energy dissipation capacity, which is a part of the total energy dissipation. The measured energy dissipation for specimens are listed in Table 5 according to the index.

It is observed from Table 5 that the energy dissipation capacity of the core wall is significantly improved by adding concealed steel truss within the core wall. Compared with specimen CWT-1, energy dissipation for the specimen CWT-2 increased 34.38%.

Table 5. Measured results of energy dissipation in first quadrant of hysteresis loop

Specimen	Total Mass of Reinforcement /kg	Mass of Concealed Steel truss /kg	Energy Dissipation /kN-mm			Relative Increase of Energy Dissipation /%
			positive	negative	average	
CWT-1	81.03	0.000	18345.23	15772.79	17059.01	0.0
CWT-2	81.03	44.48	24950.35	20898.90	22924.63	34.38

3.5 Failure Mode

Crack patterns at Failure for two specimens are illustrated in Figure 7. In the core wall, the wall which subject to the add stress of shear and torque call shear wall 1, the wall which subject to the subtractive stress of shear and torque call shear wall 3, the wall which subject to tension as horizontal load is pull called shear wall 2, the wall which subject to tension as horizontal load is pull called shear wall 2, the wall which subject to compressive stresses as horizontal load is push called shear wall 4.

From observations of the failure mode of each specimen, it is seen that the mechanical model for calculating its load-carrying capacity could be consider as shear and torque members.

Compared with the normal core wall, the concrete cracks in the core wall with concealed steel truss are tinier, closer, more in number and distribute over a larger area.

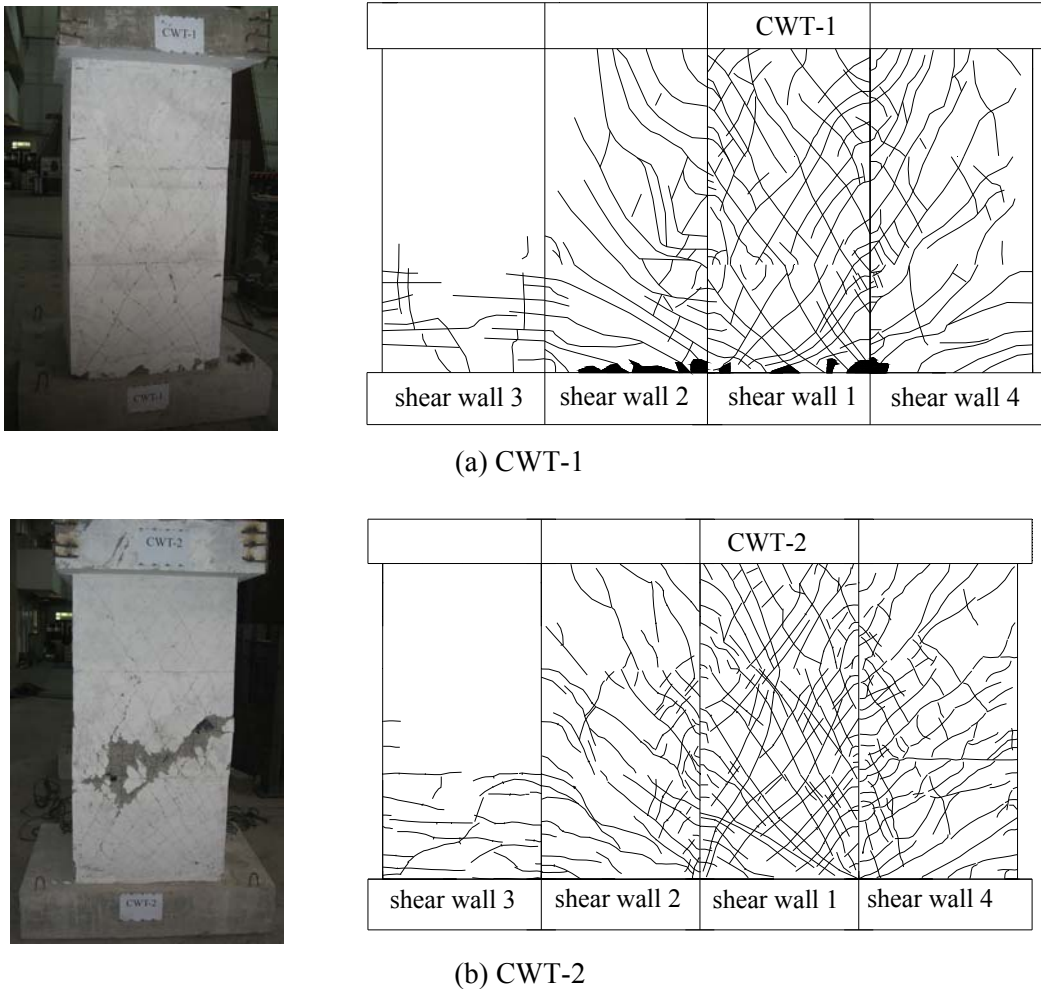


Fig.7 Mode of failure for core walls specimens

4. THEORETICAL MODEL

Based on the rotating-angle softened truss model theory, this paper presents a three-dimensional model for analysis of reinforced concrete composite core walls with concealed steel truss subjected to complex loading. Under combined action of compression, bending moment, shear and torque, each element of the section of core walls is subjected to two systems of stresses separately, including a one-dimensional stress system and a two-dimensional stress system. The one-dimensional stress system called system 1 resisted the longitudinal stresses due to compression, bending moment, shear and torque, and the two-dimensional stress system resists the shear stress due to shear and torque. The two-dimensional stress system called system 2 resists the shear

stress due to torsion and shear. The two stress systems are combined through the compatibility equations and the equilibrium of stresses in the longitudinal direction.

4.1 two-dimensional stresses (system2)

The four walls are tied together by the requirements of equilibrium of shearing stresses. The shear flow q_1 within

$$\text{the section of shear wall 1 is given by } q_1 = \frac{T}{2A_{cor}} + \frac{V}{2h_{cor}} \quad (1)$$

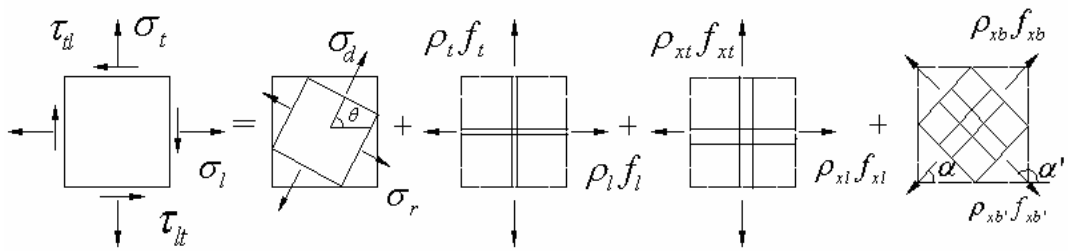
Where T is the torsion the section resisted; V is the shear the section resisted; A_{cor} is the area enclosed by the shear flow and $A_{cor} = b_{cor}h_{cor}$; and $b_{cor} = b - 2a - d_1$, $h_{cor} = h - 2a - d_1$; b and h are respectively, the wide and depth of the section of core wall ; d_1 is diameter of stirrups ; a is the concrete cover depth.

$$\text{The shear flow } q_2 \text{ within the section of shear wall 2 is given by } q_2 = \frac{T}{2A_{cor}} \quad (2)$$

$$\text{The shear flow } q_3 \text{ within the section of shear wall 2 is given by } q_3 = \frac{T}{2A_{cor}} - \frac{V}{2h_{cor}} \quad (3)$$

$$\text{The shear flow } q_4 \text{ within the section of shear wall 4 is given by } q_4 = \frac{T}{2A_{cor}} \quad (4)$$

Considering the equilibrium of the shear element, the following equations can be obtained by transforming the concrete principal stresses and bracing of truss stress into horizontal and vertical coordinate system and superimposing them with the tensile stresses of the steel reinforcement and steel, which are shown in Figure8.



(a) shear element (b) concrete (c) steel reinforcement (d) steel (e) steel bracing

Fig.8 Stresses in element of shear wall with concealed truss

$$\sigma_{li} = \sigma_{di} \cos^2 \theta_i + \sigma_{ri} \sin^2 \theta_i + \rho_{sli} \sigma_{sti} + \rho_{xli} \sigma_{xti} + \rho_{xbi} \sigma_{xbi} \cos^2 \alpha + \rho_{xbi'} \sigma_{xbi'} \cos^2 \alpha' \quad (5)$$

$$\sigma_{ti} = \sigma_{di} \sin^2 \theta_i + \sigma_{ri} \cos^2 \theta_i + \rho_{xbi} \sigma_{xbi} \sin^2 \alpha + \rho_{xbi'} \sigma_{xbi'} \sin^2 \alpha' \quad (6)$$

$$\tau_{li} = (-\sigma_{di} + \sigma_{ri}) \sin \theta_i \cos \theta_i - \rho_{xbi} \sigma_{xbi} \sin \alpha \cos \alpha - \rho_{xbi'} \sigma_{xbi'} \sin \alpha' \cos \alpha' \quad (7)$$

$$q_i = \tau_{li} t_{di} \quad (8)$$

$$N_{(v+t)_i} = \sigma_{ti} \cdot h_i \cdot t_{di} \quad (9)$$

Where σ_{li}, σ_{ti} are normal stresses in the l_i and t_i directions, respectively; τ_{lti} is shear stress in the l_i-t_i coordinate; σ_{di}, σ_{ri} are principal stresses in the d_i and r_i direction, respectively; α is the angle of inclination of the d-axis with respect to l_i -axis; θ is the angle of inclination of the bracing of truss with respect to l -axis; ρ_{sli}, ρ_{sti} are reinforcement ratios in the l and t directions, respectively; $\sigma_{sti}, \sigma_{sli}$ are steel reinforcement stress in the l and t directions, respectively; ρ_{xli}, ρ_{xti} are steel ratios in the l and t directions, respectively; $\sigma_{xti}, \sigma_{xli}$ are steel stress in the l and t directions, respectively; ρ_{xbi}, σ_{xbi} are bracing steel ratios and bracing steel stress in α direction, respectively, and $\rho_{xbi} = \frac{A_{xbi}}{b_i \cdot h_i \sin \alpha}$; $\rho_{xbi'}, \sigma_{xbi'}$ are bracing steel ratios and bracing steel stress in the α' direction, $\rho_{xbi'} = \frac{A_{xbi'}}{b_i \cdot h_i \sin \alpha'}$. t_i is effective thickness of shear flow of core wall section.

The two-dimensional compatibility condition can now be derived for the reinforced-concrete membrane elements subjected to shear and normal stress as shown in Fig.8. Using the principle of transformation of strain, the compatibility equations can be obtained as follows:

$$\varepsilon_{li} = \varepsilon_{di} \cos^2 \theta_i + \varepsilon_{ri} \sin^2 \theta_i \quad (10)$$

$$\varepsilon_{ti} = \varepsilon_{di} \sin^2 \theta_i + \varepsilon_{ri} \cos^2 \theta_i \quad (11)$$

$$\gamma_{lti} = 2(-\varepsilon_{di} + \varepsilon_{ri}) \sin \theta_i \cos \theta_i \quad (12)$$

Where $\varepsilon_{li}, \varepsilon_{ti}$ are average normal strains in l_i and t_i directions, respectively; γ_{lti} is average shear strains in the l_i-t_i coordinate; $\varepsilon_{di}, \varepsilon_{ri}$ are average principal strains in the d_i and r_i directions, respectively, (positive for tension).

$\varepsilon_{xbi}, \varepsilon_{xbi'}$ are the bracing strains in the in the direction α and in the α' direction, respectively, given by

$$\varepsilon_{xbi} = \varepsilon_{li} \cos^2 \alpha + \varepsilon_{ti} \sin^2 \alpha + \frac{1}{2} \gamma_{lti} \sin 2\alpha \quad (13)$$

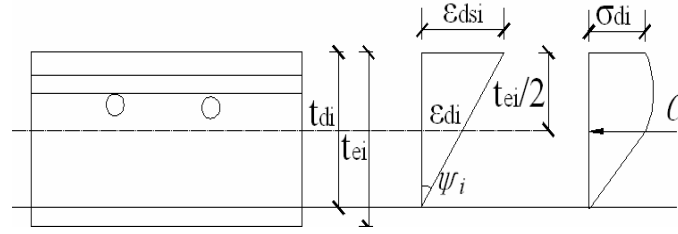
$$\varepsilon_{xbi'} = \varepsilon_{li} \cos^2 \alpha' + \varepsilon_{ti} \sin^2 \alpha' + \frac{1}{2} \gamma_{lti} \sin 2\alpha' \quad (14)$$

According to Bredt's theory, the angle of twist ϕ is given by $\phi = \oint \gamma ds / 2A_{cor} = \sum_1^4 \gamma_{ti} h$ (15)

the curvature of the concrete strut ψ_i and the angle of twist ϕ of member are related

$$\psi_i = \varphi_i \cos^2 \theta_i + \phi \sin 2\theta_i \quad (16)$$

As shown in Fig.9, the thickness of the wall is designated as t_{ei} , however, due to the bending of the concrete struts, a certain portion of the area near the bottom edge may be in tension. This tensile area will be neglected. The portion of the area that is in compression will be considered as effective. The depth of this effective area is designated t_{di} . If the strain distribution within the effective depth t_d is assumed to be linear, then the maximum compressive strain ε_{dsi} at the surface can be written as $\varepsilon_{dsi} = -\psi_i t_{di}$ (17)



Unit width of concrete strut strain diagram actual stress block

Fig. 9 Bending of concrete struts

The average of compressive stress of diagonal concrete strut is giving by

$$\sigma_d = \int_0^{\varepsilon_{ds}} f'_c(\varepsilon_d, \varepsilon_r) d\varepsilon_d / \varepsilon_{ds} \quad (18)$$

4.2 one-dimensional stresses (system1)

The longitudinal stresses in the section must be in equilibrium with the applied axial force and biaxial moment. Since torsion and shearing force cause additional longitudinal stresses in the section, their contribution must also be taken into account. The concrete, reinforce and steel stresses obtained from strain distribution over the section, and using the material constitutive laws, when integrated over the section, should add up to the sectional force. Hence

$$N + \sum_1^4 \sigma_{ti} t_{ei} b_i = \int_{A_c} \sigma_c dA_c + \int_{A_s} \sigma_s dA_s + \sum_1^2 \sigma'_{xc} A'_{xc} \sin \theta + \sum_1^2 \sigma_{xz} A_{xz} \quad (19)$$

$$M + \sum_1^4 \sigma_{ti} t_{ei} b_i x_{ci} = \int_{A_c} \sigma_c y dA_c + \int_{A_{si}} \sigma_{si} y_{si} dA_{si} + \int_{A_{xi}} \sigma_{xi} y_{xi} \sin \theta dA_{xi} + \sum_1^4 \sigma_{xzi} A_{xzi} y_{xzi} \quad (20)$$

4.3 interaction between systems 1 and 2

Links between the two idealized systems are the longitudinal strains ε_i and longitudinal forces due to shear and torsion. Hence, each wall is subjected to a shear force and a longitudinal strain ε_i . equations of the modified compressions field theory can then be used to solve for complete state of stress and strain in each wall.

The strain ε_{ti} can be computed as follow: $\varepsilon_{cen} = \varepsilon_{ti} + \varphi y$ (21)

Where ε_{cen} is the longitudinal strain at section centric, taken positive if tensile.

4.4 solutions and result

A trial-and-error method can be used as follow: 1. Select ϕ and assume $\varepsilon_{cen}, \varphi, t_i, \theta_i$; 2. Calculate ψ_i from Eq.(16); 3. Calculate ε_{dsi} from Eq.(17); 4. Calculate ε_{ti} from Eq.(21); 5. Calculate $\varepsilon_{ri}, \varepsilon_{li}, \varepsilon_{xbi}, \varepsilon_{xbi'}$ from Eq.(10)~(14); 6. Calculate σ_{di} from Eq.(18); 7. Using the Vecchio-collins stress-strain relationship of concrete calculate σ_{ri} ; 8. Using the constitutive of steel calculate $\sigma_l, f_t, f_{xl}, f_{xt}, f_{xb}, f_{xb'}$; 9. Check θ_i by (5); 10. Calculate σ_{ti} from Eq.(6); 11. Calculate τ_{li} from Eq.(7); 12. Calculate q_1 from Eq.(1); 13. Check t_i by Eq. (2) ~ (4); 14. Calculate γ_{li} from Eq.(12); 15. Check t_1 by Eq. (16); 16. Check φ by Eq. (19); 17. Check ε_{cen} by Eq. (19); 18. get T, ϕ .

The torque-twist curves for two specimens are plotted in Fig.10. Through the results of calculation coincided with the test well, this model can predict the ultimate strength of the load-carrying capacity of reinforced concrete composite core walls with concealed steel truss, and provide a tool to obtain the entire load-deformation history.

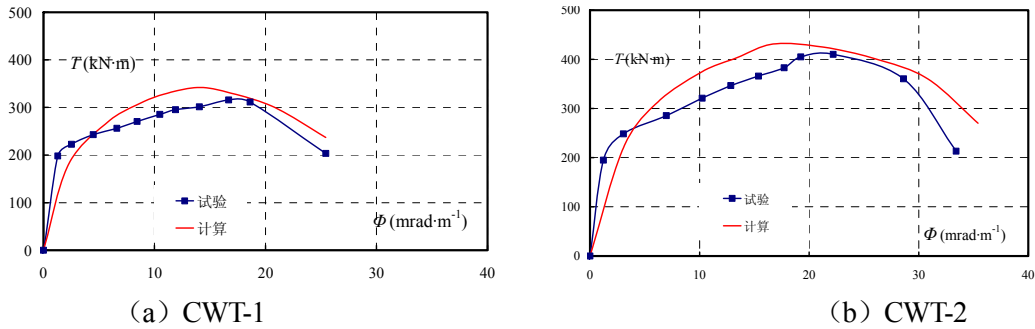


Fig. 10 Torque twist curve of subjected to core wall

5. CONCLUSIONS

A new type of core wall with concealed steel truss has been proposed and investigated. Two core wall specimens are designed and a detailed experimental investigation is carried out. The experimental results show that concealed steel truss affects not only the load-carrying capacity, stiffness and ductility, but also the mode of failure. From the experiments, it is concluded that:

(1) Core wall with concealed steel truss can display a significant increase in load-carrying capacity, stiffness in later stages of loading, ductility, and energy dissipation capacity compared with a normal core wall without concealed steel truss.

(2) Compared with the concrete cracks in normal core wall, the concrete cracks in core wall with concealed steel truss are closer and more in number, width of which is tinier.

(3) Through the results of calculation coincided with the test well, a three-dimensional model this paper presented can predict the ultimate strength of the load-carrying capacity of reinforced concrete composite core walls with concealed steel truss subjected to complex loading, and provide a tool to obtain the entire load-deformation history.

REFERENCES

- CAO Wan-lin, XUE Su-duo, ZHANG Jian-wei. (2003). Seismic Performance of RC Shear Wall with Concealed Bracing. *Advances in Structural Engineering*, **6** : 1,1-13.
- CAO Wan-lin, DONG Hong-ying, HU Guo-zhen. (2004). Seismic behavior of RC coupled shear wall with concealed bracings and its control effect for failure mechanism. *Journal of Building Structure*, **25**:3,22-28.
- CAO Wan-lin, HUANG Xue-ming, LU Zhi-cheng. (2005). Experimental study on seismic behavior of reinforced concrete core walls with concealed bracings. *Earth Quake Engineering and Engineering Vibration*, **25**:3, 81-86.
- CAO Wan-lin, ZHANG Jian-wei, TAO Jun-ping, et al. (2007). Seismic Performance Comparison Between Shear Wall with Concealed Steel Truss and Steel Truss, *Journal of BeiJing University of Technology*, **33**:1,31-36
- Anwar Hossain, K.M, Wright, H.D. (2004). Experimental and theoretical behavior of composite walling under in-plane shear. *Journal of Constructional Steel Research*. **60**:1, 59-83.
- Driver, Robert G., Kulak, Geoffrey L. et al. (1998). FE and simplified models of steel Plate shear wall. *Journal of Structure Engineerings*, **124**:2,121-130.
- Hossain, Khandaker M. Anwar. (2004). Design Aspects of Double Skin Profiled Composite Framed Shear Walls in Construction and Service Stages. *ACI Structural Journal*. **101**:1,94-102.